Bulletin of Electrical Engineering and Informatics
Vol. 8, No. 3, September 2019, pp. 777~788
ISSN: 2302-9285, DOI: 10.11591/eei.v8i3.1501

Design, simulation and practical experimentation of miniaturized turbine flow sensor for flow meter assessment

Salami Ifedapo Abdullahi, Mohamed Hadi Habaebi, Noreha Abd Malik
Department of Electrical and Computer Engineering, International Islamic University Malaysia, Malaysia

Article Info

Article history:

Received Feb 28, 2019
Revised May 2, 2019
Accepted May 17, 2019

Keywords:

3D printed sensor
Arduino
DC motor
Matlab simulink
Photo-interrupter
Solidwork flow simulation
Turbine flow sensor

ABSTRACT

Flow sensors are very essential in many aspects of our daily lives. Many of the industrial processes need a very consistent flow sensor to monitor and check for irregularities in their system. Therefore, flow sensor is an important tool for advanced operation in industrial environment. In this paper, the design and development of a 3D fabricated flow sensor was carried out using SolidWork 3D CAD. SolidWork Flow Simulation was used to model the effect the turbine flow sensor would have on a constant flowing water while MATLAB Simulink flow graph was created to visualize the effect of turbine flow sensor response with voltage input. Afterwards, the design was 3D printed using UP Plus 2 3D printer. The experimentation involved selection of sensors, coding to control the turbine flow sensor and automatic data logging and storage. During the design phase, the sensors and actuators were assembled using locally sourced material. Subsequently, under controlled laboratory environment, the turbine flow sensor was tested using a DC motor which was programmed to control the revolution per minute(rpm) of the turbine flow sensor. The rpm and velocity of the turbine flow meter was measured and stored in a database via Microsoft Excel using Cool Term Software. A total number of 517 readings were analysed to evaluate the performance of the turbine flow sensor. The result shows that the turbine flow meter is responsive to the motor input voltage and yielded accurate measurement of rpm and velocity of turbine flow meter.

Corresponding Author:

Mohamed Hadi Habaebi,
Department of Electrical and Computer Engineering,
International Islamic University Malaysia (IIUM),
Jalan Gombak, Kuala Lumpur, 53100, Malaysia.
Email: habaebi@iium.edu.my

1. INTRODUCTION

This article is an extension of the work presented during the ICCCE'18 Conference in September 2018. This article provides more comprehensive details on the previous work as the study developed further by accessing the performance of the 3D printed flow sensor. The usage of flow sensor ranges from basic home tap water flow measurement to large scale industrial liquid and mixture flow measurements. Precision and durability of flow sensor are important aspect to consider for either industrial usage or research-based usage. Historically, the Sumerian cities which their existence dated back to 5000 B.C measured water flow by utilizing buckets and a timer [1]. The method adopted by the Sumerians was to measure the time taken for flowing water to fill a known capacity of a bucket is taken while manual computation of flow rate is approximated and recorded [1]. In 1870, Benjamin G. Hoffman recorded the first use of turbine flow sensor in Hamburg, Germany by publishing a brochure describing Reinhard Woltman invention of a current meter for measuring water and air flow as shown in Figure 1 [2]. The advancement of technology in the 21st century has introduced new methods of flow sensor such as optical flow meter, thermal and mechanical flow sensors.

Researchers have heavily investigated on different mechanical flow sensors in [3-6] which are used to detect velocity of water current. [6] used a mechanical flow sensor to get the inflow rate of water entering the inlet canal while investigating the performance of the flow sensor in detecting the correct flow rate. Unlike mechanical flow sensors, thermal flow sensors used thick film segmented thermistor to sense heat changes corresponding to different flow velocity [7]. However, Magnetic flow sensors have not been able to be established well in the ever-growing technology industry as their magnetic characteristics makes the reading of the sensor to be inaccurate when it is used near areas that have high magnetic fields or elements [8]. Acoustic sound waves were being used in [9, 10] to with an effective signal processing capable machines or software that enables detection of flow rate easily. Microelectromechanical system (MEMS) sensors have paved way into the technology market and are preferred due to their capability in [8, 11] of using Nano-materials for optically assisted digital cameras and accelerometer for acquiring signals that corresponds to moving fluid flow rate.

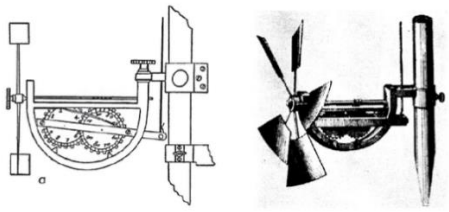

Figure 1. Original form of the Waltman meter [1]

In [12], they conducted a simulation on turbine flow sensor and its ability to detect flowing water. The turbine flow sensor was analysed on its consistency as well as the reliability of the theoretical models in which governs the method the flow sensor works. [13] utilised an ultrasonic sensor to find the right frequency which could penetrate composite pipeline to check for the irregularities in the smooth flowing of multiphase liquid. This shows another specialized method to use flow rate sensor for an industrial environment. [14] used a different approach to enable liquid level to be measured using printed circuit board. this adds an insight in different ways to integrate water flow sensor and liquid level sensor for a system. [15] used water-pump motor to control the inflow of water in an indoor vertical farming environment. The use of soil moisture with a water-pump motor enable a systematic design of an effective vertical farming which is an integrative application involving flow rate measurement.

In [16], they adopt a motor-driven system which enable cleaning of high-rise building safe and efficient. The application used a motor to maintain the amount of water outage which showed the significance of a motor in aiding water flow control systems in many different applications and fields. However, [17] investigated on Long Range (LoRa) Low Power Wireless Area Network (LPWAN) in its adaptability for Internet of Things system which the flow sensor application can be further extended. Therefore, the tremendous effort to make flow sensor integrative with many systems and applications can be made more robust by using LoRa and LPWAN which enable autonomous control of systems with less manual labour involved. These are the current investigation on flow rate sensors and the specific used in current research work and industrial aspect as well.

Flow sensors have to be compact and easy to integrate with other sensors which is the reason miniaturized flow sensors designs have been carried out in this study. This aim of this paper is to develop a system whereby turbine flow sensor can be integrated in for continuous flow rate measurement. Analyses of the turbine flow sensor will be carried out by using simulation approach and practical laboratory experiment approach as well. Finally, the 3-D printed flow sensor was assembled and tested in a controlled laboratory to access its performance. The research methodology section gives insight into the simulation steps and practical phase. Then, the result analysis section is followed by conclusion section for this paper.

2. RESEARCH METHOD

2.1. Design and fabrication of turbine flow sensor

3D CAD Software are necessary for the sketching and assembly of the turbine flow sensor [12]. SolidWorks 2015 3D CAD Software is the software enabler that was used in the design of the turbine flow sensor in the integrated design environment. The complete drawing of the turbine flow sensor can be seen in Figure 2. The drawing of the turbine flow sensor was guided by few dimensions which were carefully chosen, and their measurement are recorded. Extrude boss and filleting were the functions used in the

software to make the 3D sketch of the turbine flow sensor possible. SolidWork enabled the assembling of the six blades, shaft and hub. A fixed angle of 60° was kept apart for the blades to be arranged around the hub. The dimensions of the turbine flow sensors are tabulated in Table 1 and those measurements were made sure it can be acceptable for the 3D printer input. To ensure smooth rotation of turbine flow sensor, six blades were optimum number of blades required. The completed 3D turbine flow sensor was saved in STL file format and the image format was uploaded into the desktop connected to the UP Plus 2 3D printer. A class of plastic filament named Acrylonitrile Butadiene Styrene-Polycarbonate (ABS-PC) was the material used to print the turbine flow sensor under test. The ABS-PC filament diameter for the UP Plus 2 3D printer is 1.75mm. generally, the colour in which the 3D printer print is in a creamy white color. The weight of the printed turbine flow sensor was 117.92 grams and 1.07 grams per cubic centimeter was the density of the turbine flow sensor.

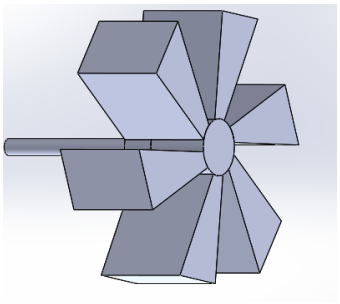

Figure 2. 3D view of turbine drawing [12]

Table 1. Dimension of turbine flow sensor parts [12]

Parts	Length of hypotenuse side (cm)	Length of adjacent side (cm)	Length of opposite side (cm)	Length (cm)	Width (cm)	Radius (cm)
Blade	4.15	3.84	2.29	-	3	-
Hub	-	-	-	3	-	1
Shaft	-	-	-	5	-	3

2.2. SolidWork flow simulation approach

The turbine flow sensor design had been imported into the Flow Simulation environment. Flow simulation event was simulated and the integrated design environment in which it was done is shown in Figure 3. Internal canal was represented by a cylinder and it encapsulate the turbine flow sensor while the external rectangular cuboid encompasses the internal canal. Dimensions of the inner canal and rectangular cuboid are given in Table 2. [18] dimensions were partially adopted, and modification were made accordingly for the design in this article. A wizard from the flow simulation tab was used to show the steps throughout the flow simulation process. Boundary condition, goals that are objectives of the flow simulation and selected medium which is water were chosen in the parameters for the flow simulation animation. The targeted objective were global goals and surface goals in this simulation. Velocity of water at 2.5m/s and 5m/s were the two-different variable of the simulation settings carried out. Thus, allowing the simulation to run its course while evaluating the effect it would have on the turbine flow sensor by choosing these two-different velocities of water

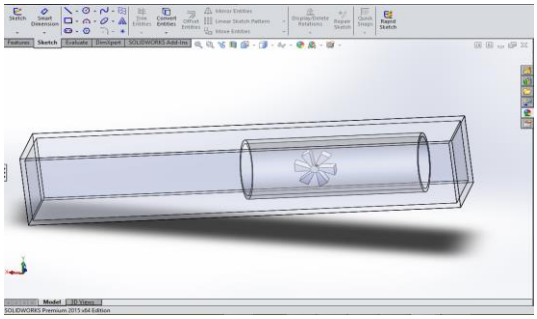

Figure 3. Pre-process before Solidwork simulation [12]

Table 2. Dimension of canal and external rectangular cuboid [12]

Components	Length (cm)	Width (cm)	Height (cm)	Radius (cm)	Thickness (cm)
Internal canal	43.7	-	-	7.2	1
External rectangular cuboid	106.5	19.41	19.54	-	1.5

2.3. MATLAB simulink simulation approach

The Simulink simulation was carried out in MATLAB R2015 Edition. DC voltage source, controlled PWM Voltage, H-Bridge, Current Sensor, Ideal rotational motion sensor, DC motor, PS-Simulink Converter and a scope were the block components utilized in this simulation [19]. Figure 4 depicts the block diagrams of the electrical circuit connection controlled PWM voltage emits pulse width modulation signal which is 4kHz while the voltage source distributes 2.5 V at every signal burst. Current sensor senses the current output, the H-bridge drives the motor and ideal rotational motion sensor senses the revolution per minutes of the motor. Armature inductance of 12V DC motor chosen in this simulation is 0.01 henry. The scope is where the result of the simulation goes to for each run.

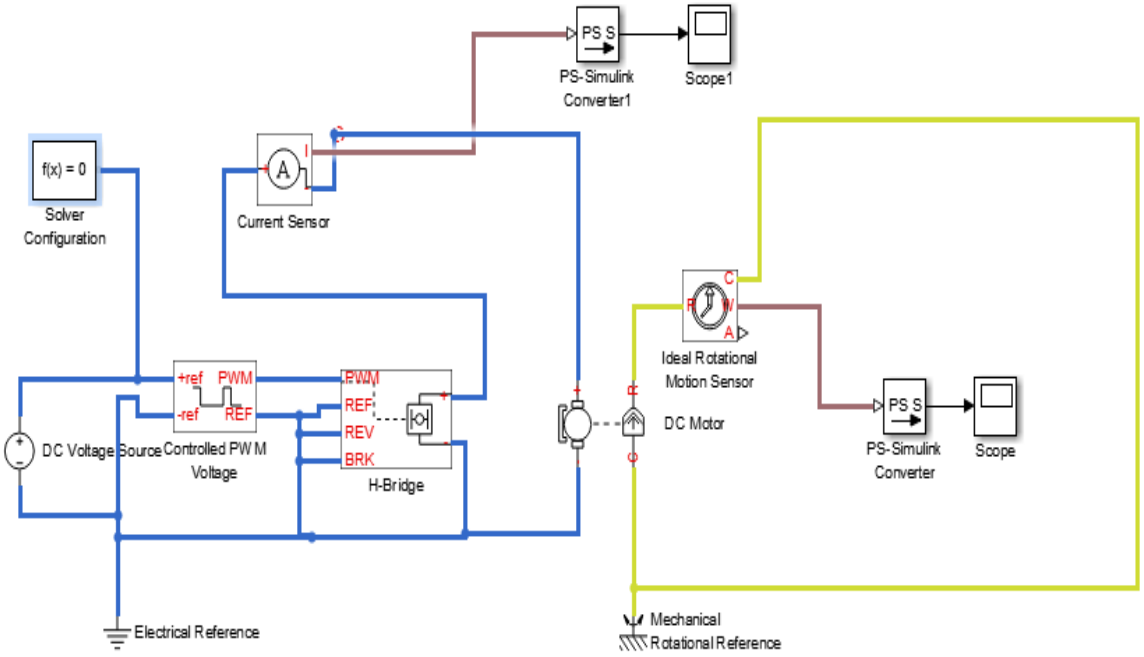

Figure 4. Block diagram of electrical block inside Simulink [12]

2.4. Performance metrics of turbine flow sensor

The schematic of the system is shown in Figure 5. Prasetyo, Budiana, Tjahjana & Hadi. (2018) [20] design approach was adopted with few modifications as shown in Figure 2. The horizontal axis water turbine of Prasetyo et al. (2018) [20] chose 6 blades as their optimum design requirement for a smooth-running water turbine. This paper also took 6 blades as a design requirement to enable smooth rotational movement. Turbine theory was employed which means rotational movement of the turbine blades is able to calculate the flow rate of moving water. A rotational force is subjected on the turbine blades as water moves pass in which energy is transferred from the flowing water to the turbine flow sensor for an effective measurement of flow rate to take place. The encoder depicted in Figure 5 which is attached to the turbine flow sensor's hub enables rotational speed measurement. The motor is connected to the microcontroller to take the readings for the linear speed of the turbine flow sensor. The DC motor was used to drive the turbine flow sensor to examine the torque and voltage requirement for tilting the fabricated flow sensor as shown in Figure 5.

Conversion of electrical energy into mechanical energy is the job of a DC motor. The electric circuit representation of the DC motor is given in Figure 6(a). E represents the input voltage when current Ia, flows through the rotor armature brushes around the circuit. The backward electromotive force emitted is directed opposite to the voltage supplied and the input into armature has resistance, Ra. Electric field and magnetic

field cross path to produce mechanical force in a DC Motor [21]. The relationship between the voltage and current flow in a DC motor is given in (1).

$$E = Eb + IaRa \quad (1)$$

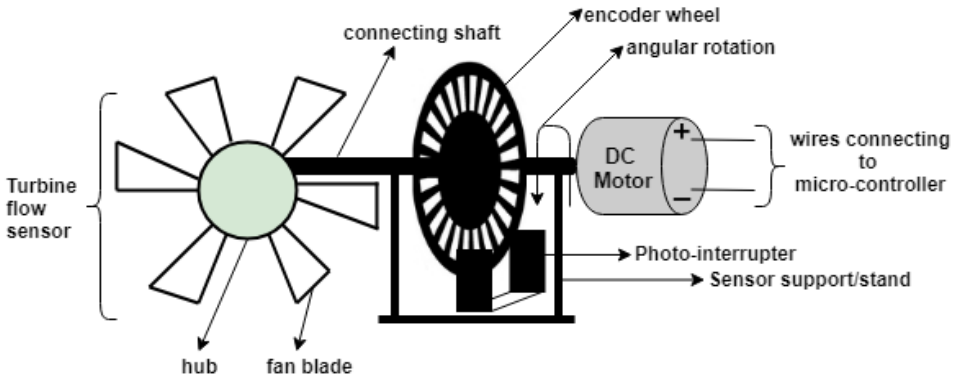

Figure 5. 2-D schematic diagram of the turbine flow sensor system

The torque formula of a DC motor is given in (2).

$$\tau = (I \times V \times E \times 60) \times (rpm \times 2\pi)^{-1} \quad (2)$$

where τ is torque, I is current flow, V is E which is voltage, E is efficiency of the motor and rpm is revolution per minute.

An encoder wheel is showed in Figure 7 and it will be used with a photo-interrupter. The electrical representation of the photo-interrupter is shown in Figure 6(b). The turbine flow sensor will be measured in revolution per minute (rpm) with the use of the photo-interrupter. Photo interrupter are an integrated device that has an upright infrared emitter and an upright shielded infrared detector (phototransistor) [22]. Photo interrupter allows electrical current to flow in it which lights up the LED and then the light enters the phototransistor while the light is converted into current. I_c is the collector current, and its expression is given in (3) to show the relationship between the base current I_b, hFE(β) and gain.

$$I_c = I_b \times hFE \quad (3)$$

(a) (b)

Figure 6. (a) DC motor electrical circuit representation, (b) electrical diagram of photo interrupter

The encoder can be depicted as the photo interrupter which enables the turbine flow sensor to get the revolution per minute. The relationship between rpm and linear velocity is given in (4).

$$velocity\left(\frac{meter}{sec}\right) = radius(meter) \times rpm\left(\frac{radian}{sec}\right) \times 2\,\pi \quad (4)$$

2.5. Selection of microcontroller, sensors and laboratory experiment

The turbine flow meter adopted the working mechanism of a motor which converts mechanical energy into electrical energy. The same concept is used on a generator as the generator(motor) in the dynamo act as the mechanical part to convert mechanical movement to electrical lighting. A photo interrupter as shown in Figure 7(a) was used to get the revolution per minute (rpm) while a 24V DC Motor (Figure 7(b)) was used to drive the turbine flow meter for experimentation purpose. The motor power outage is 1.61 Watts and it has a stall torque of 0.0188N.m. The photo interrupter acts as the encoder for the turbine flow meter to get the rpm [3]. The relationship between rpm and linear velocity is given in (4). The unit of linear velocity is usually in metre/sec, but the experimentation carried out used metre/min for a better resolution.

The motor is powered by an Arduino Uno (Figure7(c)) which can only output 40mA for each digital input and output pins. The digital input and output pins of the Arduino were used to control the voltage input for the motor. The voltage used were divided into 5 segments which were 5, 10, 15, 20 and 24 volts respectively. The motor was programmed to convert the reference voltage Arduino used which is between 0 to 255. The reference voltage was divided into equal voltages of 5, 10, 15, 20 and 24 which are 53.125, 106.25, 159.375, 212.5 and 255. The photo-interrupter which is an optical rpm sensor is programmed to respond to the encoder wheel as shown in Figure 7(d) rotation that has slots which allows for light to pass through it. The slot is the point where the photo interrupter calculates the number of turn and reads rpm of the turbine flow meter. The encoder wheel has 20 slots and a radius of 1.25 centimeter.

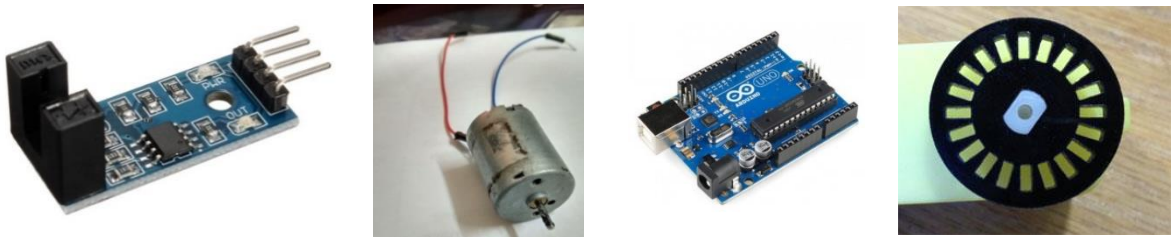

(a) (b) (c) (d)

Figure 7. (a) photo interrupter, (b) 24 VDC motor, (c) Arduino Uno, (d) Encoder wheel

The shaft of the turbine flow meter is inserted into the hole in the center of the encoder wheel to calculate the linear velocity in this experiment. The Motor was firmly attached to a rectangular box which has dimensional size of 15×15×5 cm as shown in Figure 8. The workflow is given in Figure 9 which showed the overall steps taken to analyze the turbine flow sensor. The flow of current coming from the voltage input to the motor provides a torque powerful enough to rotate the turbine flow meter which rotates the encoder wheel and Arduino records the rpm of the turbine flow meter along with its linear velocity. The calculated output torque of the motor for 15V, 16V, 20V and 24V is 0.091 N.m, 0.0521N.m, 0.025N.m and 0.023N.m respectively. The torque decreases with increasing voltage because the Arduino Uno 5V regulator controls the current coming from the USB port or the power source. The voltage input increases the rotational speed(rpm) of the motor while the current drawn by the motor increase output torque of the motor.

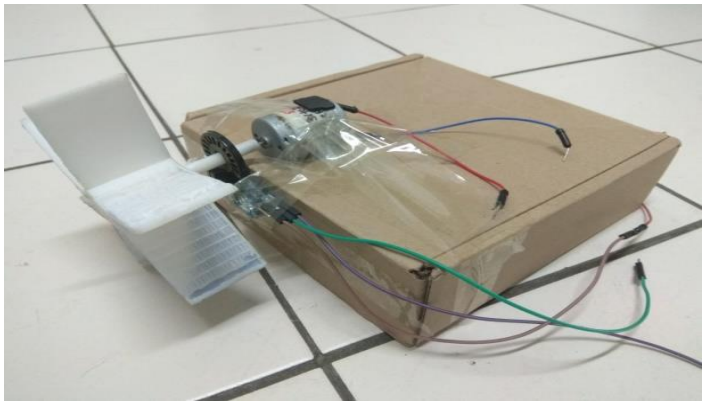

Figure 8. Experiment environment

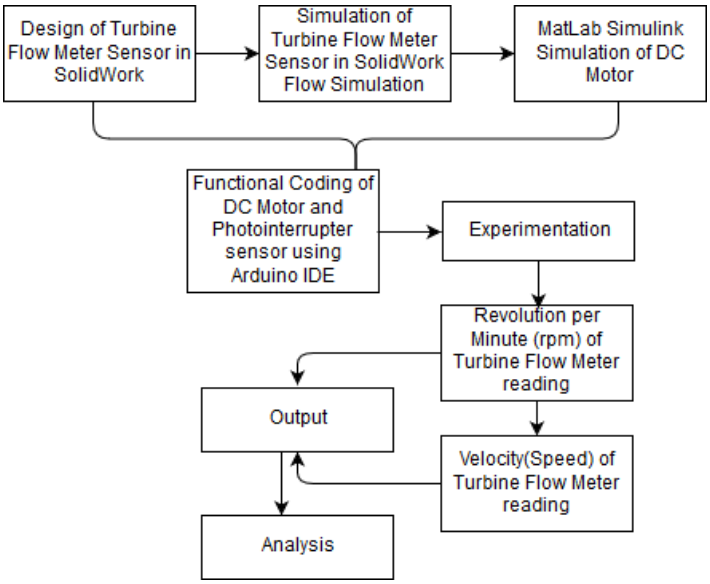

Figure 9. Workflow diagram

3. RESULTS ANALYSIS and DISCUSSION

3.1. Result analysis of SolidWork flow simulation

Flow trajectories results of water in the flow simulation is discussed in this section as well as the response of the turbine flow sensor during the simulation period. The targeted goal of this simulation is primarily to give the global goal velocity and surface goal volume flow rate. As a means of obtaining successive closer approximations for the flow simulation, the simulation process for the two-different velocities of water went through 108 iterations. To show the degree of velocity at the point where the water meets the turbine flow sensor a heat map was used in the simulation. The trajectory length represents the length of the canal. Figure 10(a) showed the flow trajectory animation which implies that the turbine flow sensor obstructed the flow of water in the canal more than the flow trajectory animation in Figure 10(b). Velocity of water set at 1.5m/s showed at Figure 11(a) implies that the increased around the turbine flow sensor was more than the turbine flow sensor's velocity of water set at 5m/s showed at Figure 11(b). These two observations match the theory that turbine flow sensor behave like an actuator and is affected by the speed at which the flow velocity collides with the water particles. A reduction was observed in the flow velocity of Figure 12(a) and Figure 12(b) after the water met the turbine flow sensor.

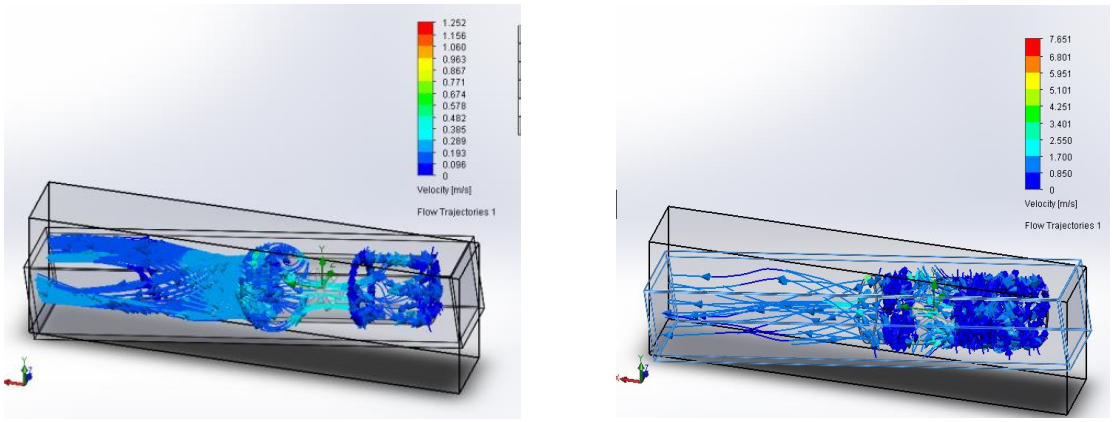

(a) (b)

Figure 10. (a) Flow trajectory animation velocity at 1.5m/s, (b) Flow trajectory of velocity at 5m/s

A 70% reduction in velocity was seen from the flow velocity set at 1.5m/s as the velocity went from 1.5 m/s to 0.8 m/s. A 10% reduction in velocity was seen from the flow velocity set at 5 m/s as the velocity went from 5 m/s to 4 m/s because of the turbine flow sensor obstruction which took place at the center of the flow trajectory. flow velocity set at 5 m/s showed lesser percentage reduction because the flow trajectory maintained a higher velocity even after the water has passed through the turbine flow sensor. the surface and global goal of the simulation were tabulated in Table 3. Overall goal of the flow simulation corresponds to the global goal while the surface goal represents the turbine flow sensor additional goal. As seen from Table 3, global goal velocity of 0.108m/s and a surface goal volumetric flow of 9.95E-5 m^3/s is realised from flow velocity set at 1.5 m/s. At the same instance, global goal of 0.983 m/s and a surface goal volumetric flow of 99.4E-5 m^3/s is pointing towards 5m/s flow velocity and these values showed a trend that was not expected but they are enough to prove that turbine flow sensor was obstructing the trajectory of the flow of water. Expression (5) showed the formula of flow rate given as:

$$\text{flow of water}(m^3/s) = \text{water velocity}(\text{m}/s) \times \text{cross sectional area}(m^2) \quad (5)$$

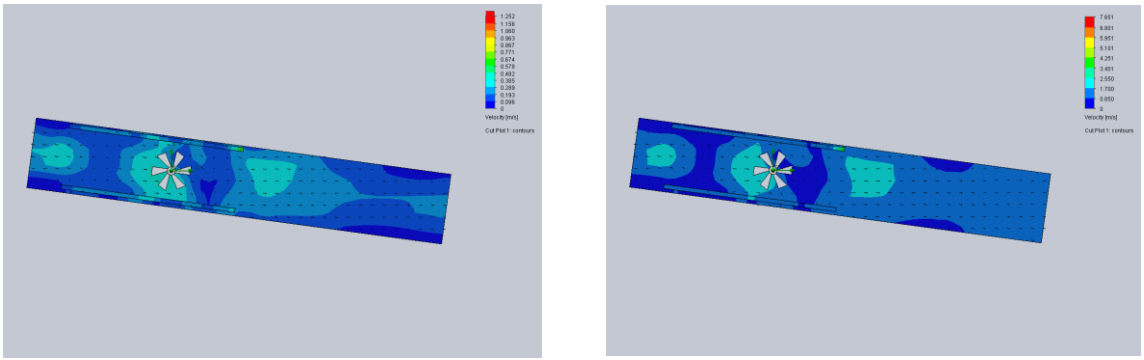

(a) (b)

Figure 11. (a) cross sectional flow trajectory of velocity at 1.5m/s, (b) cross sectional flow trajectory of velocity at 5m/s

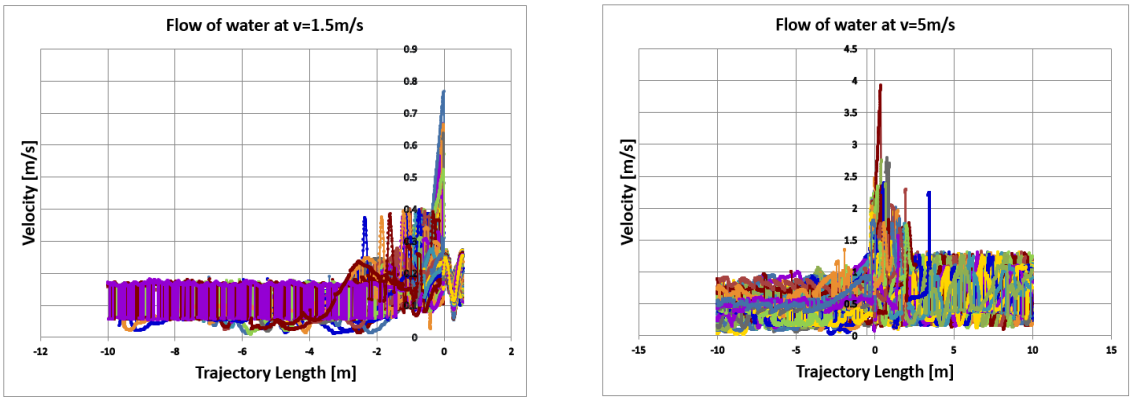

(a) (b)

Figure 12. (a) Flow trajectory plot of velocity at 1.5m/s, (b) Flow trajectory plot of velocity at 5m/s

Table 3. Simulation Result of flow velocity at 1.5m/s and 5m/s [12]

Simulation result for fixed velocity at 1.5m/s					
Goal Name (X direction)	Unit	Value	Averaged Value	Minimum Value	Maximum Value
Global Goal Velocity	[m/s]	0.102882	0.108431375	0.10288216	0.117768839
Surface Goal Volume Flow Rate	[m^3/s]	4.57e-06	9.95e-05	-0.000144392	0.000301166
Simulation result for fixed velocity at 5 m/s					
Goal Name	Unit	Value	Averaged Value	Minimum Value	Maximum Value
Global Goal Velocity	[m/s]	0.983866	0.982595626	0.972413984	1.018583914
Surface Goal Volume Flow Rate	[m^3/s]	0.001381	0.000994398	-0.001431613	0.002485519

3.2. Result analysis of simulink simulation

Two plots from the Simulink simulation were achieved as shown in Figure 12. A rapid increment in speed from 0 rad/s to 200 rad/s was seen in Figure 13(a) when 2.5 volts is supplied to the 12 VDC motor. A reduction in current output of the motor from 1.5 A to 0 is depicted in Figure 13(b). A maximum rpm of 2000 rad/s was only able to be reached because the voltage supplied is limited to only 2.5V only. However, the current output started with a maximum output current of 1.5 A and ended with 0 A because there is a transient response at the H-bridge at the instant when eelectromotive force burst occurred. The effect of transient response on the motor can be seen when the motor is supplied with voltage which is depicted at the current plot. Thus, this result validates the flow simulation the turbine flow sensor in Figure 2 will get an electrical response when flowing water comes in contact with it.

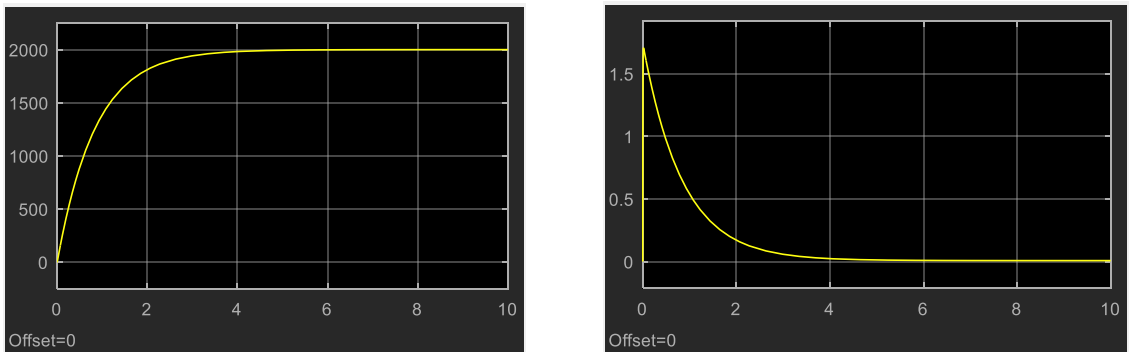

(a) (b)

Figure 13. (a) simulation output of motor rpm against time, (b) simulation output of motor current and time

3.3. Result analysis of test conducted on the fabricated flow sensor

The data from the experimentation was recorded with CoolTerm Software which connects to the input port of Arduino Uno. The data from the Coolterm software was exported into Microsoft Excel 2010 for further data analysis. Table 4 showed 80 out of 517 raw data in Excel with two rows, rpm and speed displaying the raw values from the practical simulation carried out using Arduino Uno. Figure 14 showed the plot for the rpm and speed of turbine flow sensor against time and Figure 15 showed the rpm against speed of turbine flow sensor. Figure 14 showed the different voltage input and the rpm and speed response respectively against the time elapsed during the experiment. The voltage applied to the flow sensor represents the force of water movement on the fan blades of the flow sensor. The plot revealed that as the voltage input increased the rpm and the speed of the turbine flow increases as well. Furthermore, Figure 14 showed that the minimum voltage to give enough torque to the motor to rotate the turbine flow sensor is 15 volts using the 24V DC motor. The average rpm recorded for 15V, 16V, 20V and 24V input voltage into the motor are 169 rad/s, 295 rad/s, 603 rad/s and 681 rad/s. The average speed in meter per min (m/min) for 15V, 16V, 20V and 24V input voltage into the motor are 13.28 m/min, 23.16 m/min, 47.39 m/min, 63.47 m/min. XLStat was used to produce the descriptive statistical analysis of the data set from the experiment. Figure 15 also represents the Linear Regression plot for the rpm against speed of the turbine flow meter. The correlation matrix from the linear regression analysis produced a coefficient of determination (R^2) of 1 and a Root Mean Square Error (RMSE) of 0. This showed that there is a strong relationship between the rpm and the speed of the turbine flow meter. Therefore, this validates the experimentation and showed that the turbine flow sensor can read flow velocity accurately.

The contribution on this research work can be seen by comparing it with [20]. It can be seen clearly that the system described in this research is a laboratory experimental testbed while [20] was only a simulation. Furthermore, the system built in this work requires less torque compare with [20] for the turbine blade. In a nutshell, this experimental test bed has tested the flow sensor ability to measure flow consistently and continuously.

Table 4. Raw data from experiment

15 volts		16 volts		20 volts		24 volts	
rpm	speed	rpm	speed	rpm	speed	rpm	speed
201	15.7785	201	15.7785	462	36.267	666	52.281
165	12.9525	255	20.0175	567	44.5095	684	53.694
186	14.601	291	22.8435	606	47.571	654	51.339
168	13.188	306	24.021	633	49.6905	678	53.223
183	14.3655	291	22.8435	633	49.6905	666	52.281
153	12.0105	300	23.55	618	48.513	678	53.223
198	15.543	303	23.7855	633	49.6905	684	53.694
156	12.246	306	24.021	624	48.984	687	53.9295
192	15.072	303	23.7855	627	49.2195	684	53.694
159	12.4815	285	22.3725	609	47.8065	663	52.04551
165	12.9525	294	23.079	624	48.984	666	52.281
150	11.775	294	23.079	600	47.1	690	54.165
186	14.601	285	22.3725	597	46.8645	690	54.165
147	11.5395	300	23.55	618	48.513	672	52.75201
186	14.601	297	23.3145	609	47.8065	678	53.223
168	13.188	294	23.079	609	47.8065	684	53.694
174	13.659	297	23.3145	648	50.868	684	53.694
162	12.717	297	23.3145	621	48.7485	693	54.40051
177	13.8945	291	22.8435	621	48.7485	690	54.165
165	12.9525	285	22.3725	603	47.3355	690	54.165

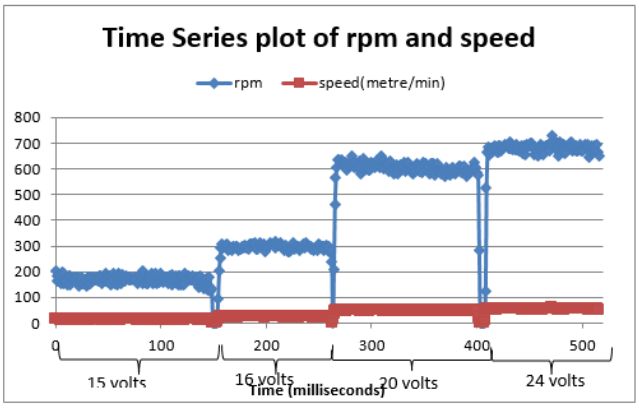

Figure 14. Time series plot of rpm and speed

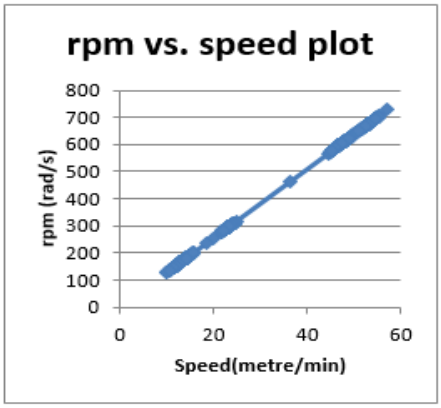

Figure 15. Plot of rpm against speed

4. CONCLUSION

A state of the art flow sensor has been designed and it usage has been practicalized by accessing its performance. Consecutively, this study has both consumed the both the simulation phase and the practical testing of the turbine flow sensor with a critical measure of the performance of the turbine flow sensor. The SoldWork 3D CAD software has made the fabrication of the turbine flow sensor possible. The flow sensor has been tested under laboratory settings and it was found that the coefficient of determination is 1 which is a strong representation of the relationship between the flow velocity and revolution per second of the motor subjected in a rotational motion. Under laboratory experiment, the turbine flow sensor performed efficiently by measuring water flow rate in a standardized environment. The mean flow rate shows strong consistency with increasing force of water applied on it. Future work will need to integrate other sensors in order to know the sensitivity of this turbine flow sensor in being able to detect flow rate readings effectively. The turbine flow sensor is still in development stage but it's ability to survive in outdoor environment would also be a very good aspect to test in the future work as well.

ACKNOWLEDGEMENTS

This work was conducted in IOT and Wireless Communication Protocols Lab, and is partially funded by IIUM Publication RIGS grant no. P-RIGS19-003-0003 and the Malaysian Ministry of Education (MOE) research fund No. FRGS16-067-0566.

REFERENCES

[1] Mays, L. W. "Water technology in ancient Egypt". *In Ancient Water Technologies. Springer*, Dordrecht. 2010. pp. 53-65.

[2] Monica, Phys & Crainic, Monica. "A Short History Of Residential Water Meters Part I Mechanical Water Meters With Moving Parts*". Installations for Buildings and Ambiental Comfort Conference XXI- edition* Timisoara – Romania. 18-20April 2012.

[3] Hughes, D., Greenwood, P., Blair, G., Coulson, G., Pappenberger, F., Smith, P., & Beven, K. "An intelligent and adaptable grid-based flood monitoring and warning system". *In Proceedings of the UK eScience All Hands Meeting*. p. 10. 2006, September.

[4] Hossain, M. E., Turna, T. N., Soheli, S. J., & Kaiser, M. S. "Neuro-fuzzy (nf)-based adaptive flood warning system for Bangladesh". *2014 International Conference on Informatics, Electronics & Vision (ICIEV)*, 2014. pp. 1-5.

[5] Abdullahi, S. I., Habaebi, M. H., Gunawan, T. S., & Islam, M. R. "Miniaturized Water Flow and Level Monitoring System for Flood Disaster Early Warning". *In IOP Conference Series: Materials Science and Engineering IOP Publishing*. Vol. 260, No. 1, p. 012019. 2017, November.

[6] Abdullahi SI, Habaebi MH, Malik NA. "Flood Disaster Warning System on the go". *In 2018 7th International Conference on Computer and Communication Engineering (ICCCE)*. 2018 Sep 19. pp. 258-263.

[7] Aleksic, O. S., Savic, S. M., Nikolic, M. V., Sibinoski, L., & Lukovic, M. D. "Micro-flow sensor for water using NTC thick film segmented thermistors". *Microelectronics International*, 26(3), 30-34. 2009.

[8] Waghmare, A., & Naik, A. A. "Water velocity measurement using contact and Non-contact type sensor". *In 2015 Communication, Control and Intelligent Systems (CCIS)*. pp. 334-338. 2015, November.

[9] Ibarz, A., Bauer, G., Casas, R., Marco, A., & Lukowicz, P. "Design and evaluation of a sound based water flow measurement system". *In European Conference on Smart Sensing and Context. Springer Berlin Heidelberg.* pp. 41-54. 2008, October

[10] Sithole, B., Rimer, S., Ouahada, K., Mikeka, C., & Pinifolo, J. "Smart water leakage detection and metering device". *In IST-Africa Week Conference IIMC*, May 2016. pp. 1-9.

[11] Xu, C., Fan, W., Qiang, Y., Liang, H., & Pan, H. "A current meter used for the estimation of water flow rate in the upwelling pipe". *In OCEANS 2016-Shanghai*. 2016, April, pp. 1-4.

[12] Abdullahi SI, Malik NA, Habaebi MH, Salami AB. "Miniaturized Turbine Flow Sensor: Design and Simulation". *7th International Conference on Computer and Communication Engineering (ICCCE)* 2018 Sep 19. pp. 38-43.

[13] Shaib MF, Rahim RA, Muji SZ. "Development of Non-Invasive Ultrasonic Measuring System for Monitoring Multiphase Flow in Liquid Media within Composite Pipeline". *International Journal of Electrical and Computer Engineering (IJECE)*. 2017 Dec 1;7(6):3076-87.

[14] S. I. Abdullahi, M. H. Habaebi and N. A. Malik, "Capacitive Electrode Sensor: Design and Testing," *2018 7th International Conference on Computer and Communication Engineering (ICCCE)*, Kuala Lumpur, 2018, pp. 34-37.

[15] Shomefun TE, Awosope C, Diagi E. "Microcontroller-Based Vertical Farming Automation System". *International Journal of Electrical and Computer Engineering (IJECE).* 2018 Aug 1;8(4).

[16] Karthik, M. S. "Automatic Skyscraper Window Cleaning System". *International Journal of Robotics and Automation (IJRA)*, 2017, 6(1): 15-20.

[17] Habaebi MH, Chowdhury IJ, Islam MR, Zainal NA. "Effects of Shadowing on LoRa LPWAN Radio Links". *International Journal of Electrical and Computer Engineering (IJECE)*. 2017 Dec 1;7(6):2970-6.

[18] Attilio Colangelo. (2016, May 5). Flow Simulation Basic Concepts. Retrieved from http://www.engineersrule.com

[19] DC Motor Model. Retrieved from https://www.mathworks.com. Retrieved on 20 June 2018

[20] Prasetyo, H., Budiana, E. P., Tjahjana, D. D. D. P., & Hadi, S. "The Simulation Study of Horizontal Axis Water Turbine Using Flow Simulation Solidworks Application". *In IOP Conference Series: Materials Science and Engineering* IOP Publishing. 2018, February, Vol. 308, No. 1, p. 012022.

[21] Pintu Singh. (2017, July 3). DC Motor or Direct Current Motor. Retrieved from https://www.electrical4u.com. Retrieved on 15 June 2018

[22] What is a Photointerrupter. ROHM Semiconductor. Retreived from http://www.rohm.com/web/global/. Retrieved on 15 June 2018.

BIOGRAPHIES OF AUTHORS

Abdullahi Salami recently acquired his Bachelor's degree in Telecommunication Engineering from International Islamic University Malaysia in 2018 and he is pursuing his Master in Telecommunication Engineering in International Islamic University Malaysia. His research interests are towards the fields of Telecommunications, Internet of Things, Data Analytics and Electronics. E-mail address:abdusalife@gmail.com

Mohamed Hadi Habaebi is with the department of electrical and Computer Engineering, International Islamic University Malaysia. His research interests are in IoT, wireless communications and Networking.

Noreha Abdul Malik received her BEng in Medical Electronics from University of Technology Malaysia (2001) and later pursued her MEng in Communication and Computer Engineering at National University of Malaysia (2004). She later received her PhD in Electronics and Electrical Engineering from University of Southampton, United Kingdom (2011). She is currently an assistant professor at International Islamic University Malaysia (IIUM). Her research interests are in biomedical signal processing and biomedical applications. She is a member of Institute of Engineers Malaysia (IEM) and Board of Engineer Malaysia (BEM).